Meccanica (2015) 50:207–216
DOI 10.1007/s11012-014-0066-z

State space reconstruction applied to a multiparameter chaos control method

Aline Souza de Paula · Marcelo Amorim Savi

Received: 7 October 2013 / Accepted: 29 September 2014 / Published online: 12 October 2014

Abstract The idea of the chaos control is the stabilization of unstable periodic orbits (UPOs) embedded in chaotic attractors. The OGY method achieves system stabilization by using small perturbations promoted in the neighborhood of the desired orbit when the trajectory crosses a Poincaré section. A generalization of this method considers multiple actuations of parameters and sections, known as semi-continuous multiparameter method. This paper investigates the state space reconstruction applied to this general method, allowing chaotic behavior control of systems with non-observable states using multiple control parameters from time series analysis, avoiding the use of governing equations. As an application of the proposed multiparameter general formulation it is presented an uncoupled approach where the control parameters do not influence the system dynamics when they are not active. This method is applied to control chaos in a nonlinear pendulum using delay coordinates to perform state space reconstruction. Results show that the proposed procedure can be applied together with delay coordinates providing UPO stabilization.

Keywords Chaos control · Nonlinear dynamics · Pendulum · State space reconstruction · Delay coordinates

A. S. de Paula
Department of Mechanical Engineering, Universidade de Brasília, Brasília, DF 70.910.900, Brazil
e-mail: alinedepaula@unb.br

M. A. Savi (✉)
Department of Mechanical Engineering, COPPE, Universidade Federal do Rio de Janeiro,
P.O. Box 68.503, Rio de Janeiro, RJ 21.941.972, Brazil
e-mail: savi@mecanica.ufrj.br

1 Introduction

Chaos is a kind of nonlinear system response that has a dense set of unstable periodic orbits (UPOs) embedded in a chaotic attractor. The idea of the chaos control is to explore the UPO stabilization obtaining dynamical systems that may quickly react to some new situation, changing conditions and their response. Chaos control may be understood as the use of tiny perturbations for the stabilization of UPOs embedded in a chaotic attractor and its methods may be classified as discrete or continuous techniques.

The first chaos control method was proposed by Ott et al. [25], nowadays known as the OGY method as a tribute of their authors (Ott–Grebogi–Yorke). This is a discrete technique that considers small perturbations promoted in the neighborhood of the desired orbit when the trajectory crosses a specific surface, such as Poincaré section [19, 33]. On the other hand, continuous methods are the so called delayed feedback control, proposed by Pyragas [28], which states that chaotic systems can be stabilized by a feedback perturbation proportional to the difference between the present and a

delayed state of the system. There are many improvements of the OGY method that aim to overcome some of its original limitations, as for example: control of high periodic and high unstable UPO [20, 24, 31], control using time delay coordinates [15, 8, 26, 34], multiparameter control [4, 10, 24]). Continuous methods also have improvements as the extended time delayed feedback control [35] and the one to improve the UPO stabilization capacity [29]. Yanchunk and Kapitaniak [36, 37] investigates continuous control of coupled systems that undergo chaos-hyperchaos transition. De Paula and Savi [12] presented a comparative analysis of some chaos control methods, investigating their performances. In brief, the conclusions point that the multiparameter approach presents better efficacy when compared with other discrete methods and also continuous approaches.

Chaos control has been applied to several dynamical systems, considering different purposes. Pyragas [29] presented several numerical and experimental applications. Ogorzalek [23], Arecchi et al. [2], Fradkov et al. [17] and Kapitaniak [21, 22] presented a general overview of chaos control methods, including discrete and continuous techniques. Andrievskii and Fradkov [1] mentioned several works that apply control procedures to numerous systems of different fields. Pereira-Pinto et al. [26] and De Paula and Savi [9–11] investigated a nonlinear pendulum as a representative example of mechanical systems. Bessa et al. [5–7] discussed sliding mode control approach in order to treat the same pendulum system. Ferreira et al. [16] discussed the application of delayed feedback control in cardiac systems. De Paula et al. [14] employed the delayed feedback control method applied to a different pendulum system employed for energy harvesting from sea waves. Chaos control and bifurcation control are successfully treated.

The semi-continuous multiparameter (SC-MP) chaos control method can be understood as a generalization of the classical OGY approach considering multiple parameter actuation and also semi-continuous perturbation (De Paula and Savi 2007). The semi-continuous perturbation introduces as many intermediate control stations as it is necessary to achieve stabilization of a desirable UPO. This paper considers the use of state space reconstruction associated with the general SC-MP chaos control method, allowing the application of this procedure in systems with non-observable states from time series analysis, avoiding the knowledge of governing equations. The method of delay coordinates are employed for this aim, implying that the controller is dependent on all control parameters perturbations performed in delayed times. Pereira-Pinto et al. [27] presented an alternative approach based on extended state observers to perform the same reconstruction for a single-parameter OGY method. As an application of the general formulation a two-parameter uncoupled control of a nonlinear pendulum is carried out. It is considered that only the scalar time series of pendulum position is available and system dynamics is reconstructed by using delay coordinates. Results show that the procedure is a good alternative for chaos control since it provides an effective UPO stabilization.

2 Multiparameter chaos control method

A chaos control method may be understood as a two-stage technique. The first step is known as learning stage where the unstable periodic orbits are identified and some system characteristics are evaluated. After that, there is the control stage where the desirable UPOs are stabilized.

The OGY approach is described considering a discrete system of the form of a map $\xi^{n+1} = F(\xi^n, p)$, where $p \in \Re$ is an accessible parameter for control. This is equivalent to a parameter dependent map associated with a general surface, usually a Poincaré section. The control idea is to monitor the system dynamics until the neighborhood of a desirable point is reached. After that, a proper small change in the parameter p causes the next state ξ^{n+1} to fall into the stable direction of the desirable point. In order to find the proper variation in the control parameter, δp, it is considered a linearized version of the dynamical system near this control point. The linearization has a homeomorphism with the nonlinear problem that is assured by the Hartman–Grobman theorem [32]. The semi-continuous control method introduces as many intermediate control stations as it is necessary to achieve stabilization of a desirable UPO. In order to use N control stations per forcing period T, one introduces N equally spaced successive Poincaré sections $\Sigma_n (n = 1,\ldots,N)$.

The semi-continuous multiparameter (SC-MP) chaos control method is a generalization of the OGY method that adopts N_p different control parameters, p_i $(i = 1,\ldots,N_p)$. By considering a specific control station, only one of those control parameters actuates.

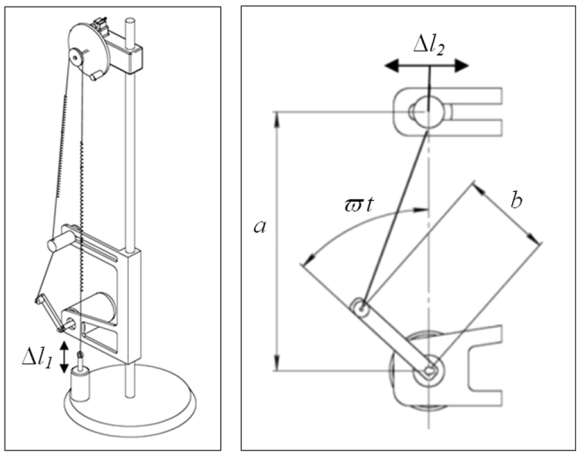

Fig. 1 Nonlinear pendulum schematic pictures

Under this assumption, the map F, that establishes the relation of the system behavior between the control stations Σ_n and Σ_{n+1}, depends on all control parameters. Although only one parameter actuates in each section, it is assumed the influence of all control parameters based on their positions in station Σ_n. On this basis,

$$\xi^{n+1} = F(\xi^n, P^n) \tag{1}$$

where P^n is a vector with all control parameters. By using a first order Taylor expansion, one obtains the linear behavior of the map F in the neighborhood of the control point ξ_C^n and around the control parameter reference position, P_0, as follows:

$$\delta\xi^{n+1} = J^n \delta\xi^n + W^n \delta P^n \tag{2}$$

where $\delta\xi^{n+1} = \xi^{n+1} - \xi_C^{n+1}$, $\delta\xi^n = \xi^n - \xi_C^n$, $\delta P^n = P^n - P_0$ is the control actuation, $J^n = D_{\xi^n} F(\xi^n, P^n)\big|_{\xi^n=\xi_C^n, P^n=P_0}$ is the Jacobian matrix and $W^n = D_{P^n} F(\xi^n, P^n)\Big|_{\xi^n=\xi_C^n, P^n=P_0}$ is the sensitivity matrix where each column is related to a control parameter. In order to evaluate the influence of all parameters actuation, it is assumed that the system response is given by a linear combination of the system responses when each parameter actuates isolated and the others are fixed at their reference value. Therefore,

$$\delta P^n = B^n \delta p^n \tag{3}$$

where B^n is defined as a $[N_p \times N_p]$ diagonal matrix formed by the weighting parameters, i.e., $\mathrm{diag}(B^n)_i = \beta_i^n$. This can be understood considering that each parameter influence is related to a vector with components $q_i = W_i^n \delta p_i^n = W_i^n \left(p_i^n - p_{0i}\right)$, and the general actuation is given by:

$$q = \beta_1 q_1 + \beta_2 q_2 + \cdots + \beta_{N_p} q_{N_p} \tag{4}$$

and β_i weights each parameter influence in the system response. Note that q may be written as follows:

$$\begin{aligned} q &= \beta_1^n W_1^n \delta p_1^n + \beta_2^n W_2^n \delta p_2^n + \cdots + \beta_{N_p}^n W_{N_p}^n \delta p_{N_p}^n \\ &= W^n B^n \delta p^n \end{aligned} \tag{5}$$

Moreover, in each control station of all N considered per forcing period, it is assumed that only one parameter actuates. Thus, it is possible to define active parameters, represented by subscript a, $\delta P_a^n = B_a^n \delta p_a^n$ (actuates in station Σ_n), and passive parameters, represented by subscript p, $\delta P_p^n = B_p^n \delta p_p^n$ (does not actuate in station Σ_n). At this point, it is assumed a weighting matrix for active parameter, B_a^n, and other for passive parameters, B_p^n. Therefore,

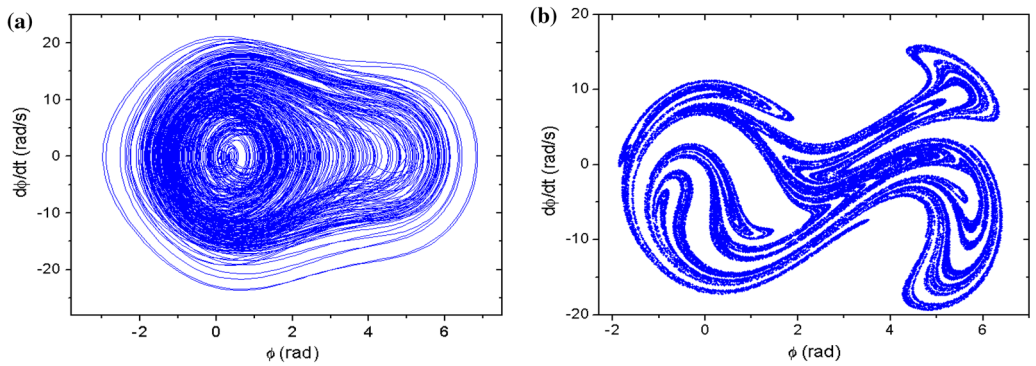

Fig. 2 System response. **a** Phase space; **b** Poincaré section

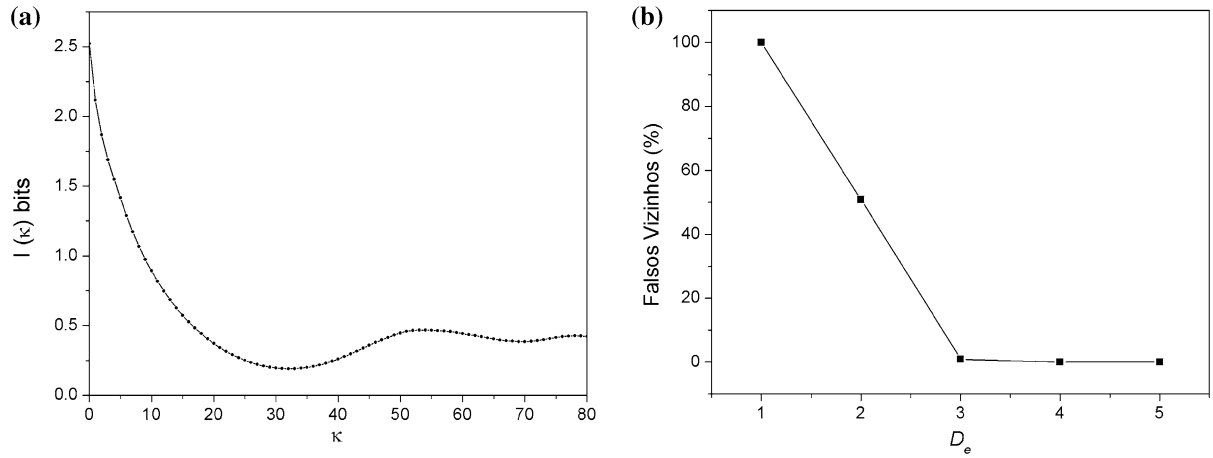

Fig. 3 Delay parameters determination. **a** Time delay, κ; **b** Embedding dimension, D_e

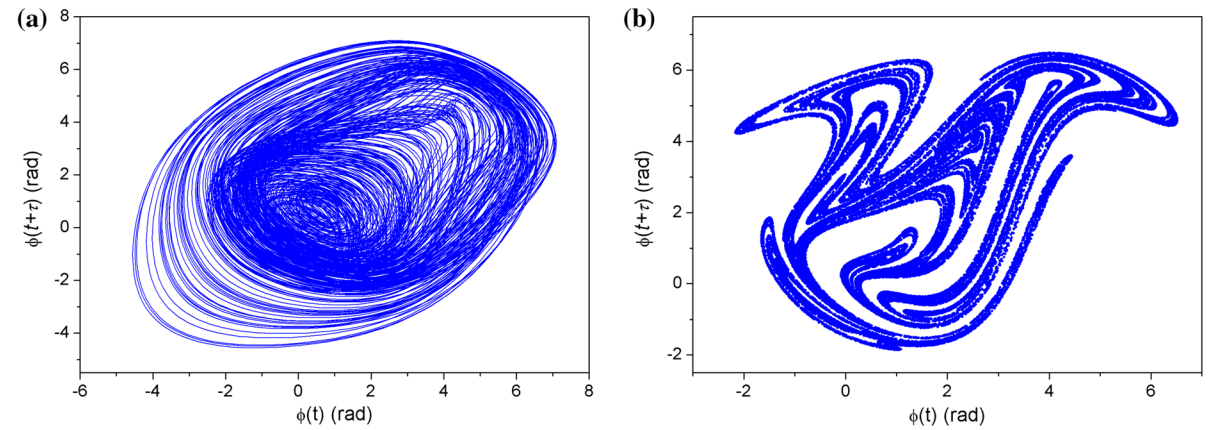

Fig. 4 Reconstructed dynamics. **a** Phase space; **b** Poincaré section

$$\delta\xi^{n+1} = J^n\delta\xi^n + W^n\delta P_a^n + W^n\delta P_p^n \tag{6}$$

Now, it is necessary to align the vector $\delta\xi^{n+1}$ with the stable direction v_s^{n+1}:

$$\delta\xi^{n+1} = \alpha v_s^{n+1} \tag{7}$$

where $\alpha \in \Re$ needs to be satisfied as follows:

$$J^n\delta\xi^n + W^n\delta P_a^n + W^n\delta P_p^n = \alpha v_s^{n+1} \tag{8}$$

Therefore, once the unknown variables are α and the non-vanishing term of the vector δP_a^n, one obtains the following system:

$$\begin{bmatrix} W^n & -v_s^{n+1} \end{bmatrix} \begin{Bmatrix} \delta P_a^n \\ \alpha \end{Bmatrix} = -\begin{bmatrix} J^n & W^n \end{bmatrix} \begin{Bmatrix} \delta\xi^n \\ \delta P_p^n \end{Bmatrix} \tag{9}$$

The solution of this system furnishes the necessary values for the system stabilization: α and δp_{ai}^n, where δp_{ai}^n is related to the non-vanishing element of the vector δP_a^n. Note that the actuation is given by: $\delta p_{ai}^n = \delta P_{ai}^n / \beta_{ai}^n$.

A particular case of this control procedure has uncoupled control parameters meaning that each parameter returns to the reference value when it becomes passive. Moreover, since there is only one active parameter in each control station, the system response to parameter actuation is the same as when it actuates alone. Under this assumption, passive influence vanishes and active vector is weighted by 1, which is represented by:

$$B_p^n = 0 \text{ and } B_a^n = I \tag{10}$$

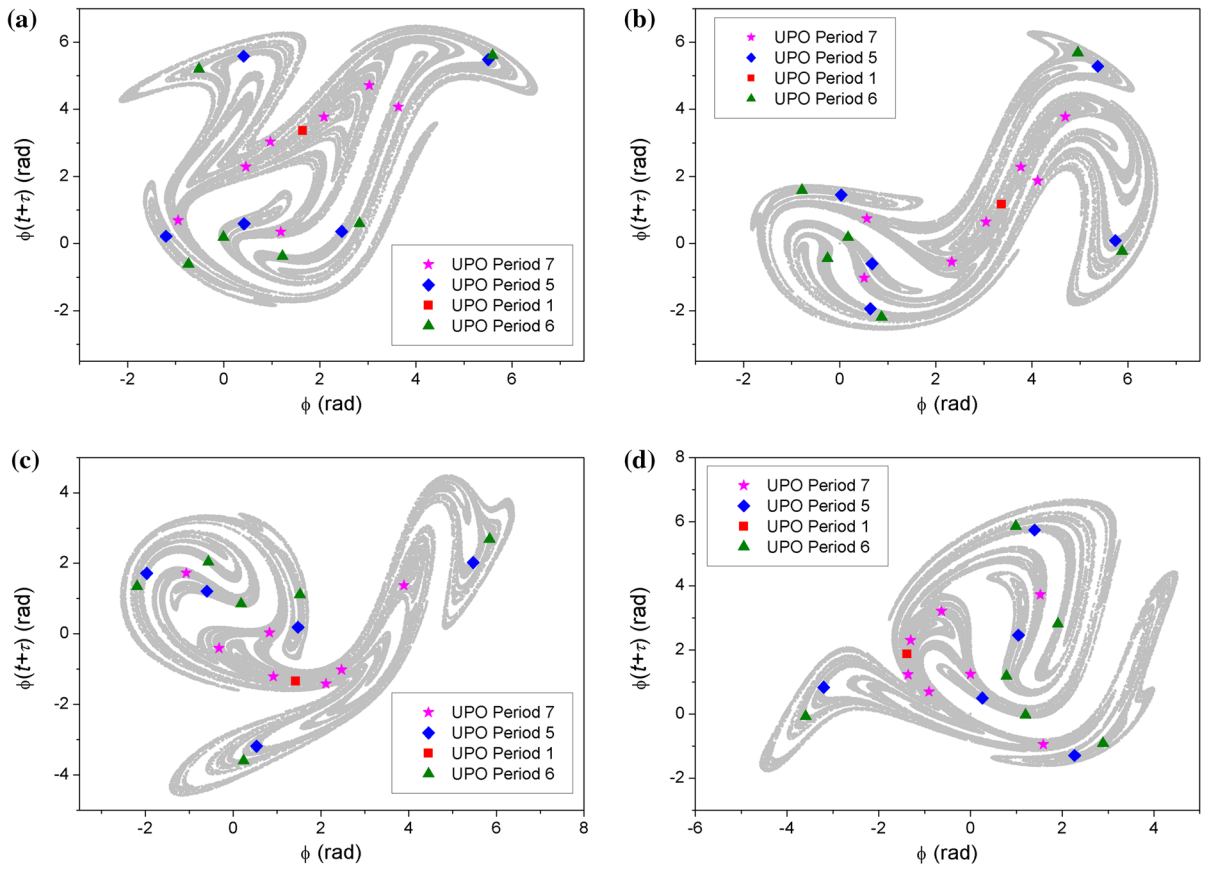

Fig. 5 UPOs to be stabilized by the control rule at: **a** S_1; **b** S_2; **c** S_3; and **d** S_4

where I is the identity matrix.

Therefore, the map F, that establishes the relation of the system behavior between the control stations Σ_n and Σ_{n+1}, is just a function of the active parameters, $\xi^{n+1} = F\left(\xi^n, P_a^n\right)$, and the linear behavior of the map F in the neighborhood of the control point ξ_C^n and around the control parameter reference positions, P_0, is now defined by:

$$\delta\xi^{n+1} = J^n \delta\xi^n + W^n \delta P_a^n \tag{11}$$

where the sensitivity matrix W^n is the same of the previous case. Since $B_a^n = I$, it follows that $\delta P_a^n = \delta p_a^n$, meaning that the value of δP_a^n corresponds to the real perturbation necessary to stabilize the system. In order to align the vector $\delta\xi^{n+1}$ with the stable direction, the following system is obtained:

$$[W^n - v_s^{n+1}] \begin{Bmatrix} \delta P_a^n \\ \alpha \end{Bmatrix} = -J^n \delta\xi^n \tag{12}$$

2.1 State space reconstruction

A time series can be understood as a time evolution of an observable variable of a dynamical system that can be a state variable or a representation of that. An essential point related to the time series analysis is that this observable variable contains all information related to the system dynamics. Therefore, the dynamics can be reconstructed by a scalar time series and there are different alternatives to perform the state space reconstruction. The method of delay coordinates may be used to construct a vector time series that is equivalent to the original dynamics from a topological point of view. The state space reconstruction needs to form a coordinate system to capture the structure of orbits in state space, which could be done using lagged variables. Then, it is possible to use a collection of time delays to create a vector in a D_e-dimensional space. The application of this approach is associated

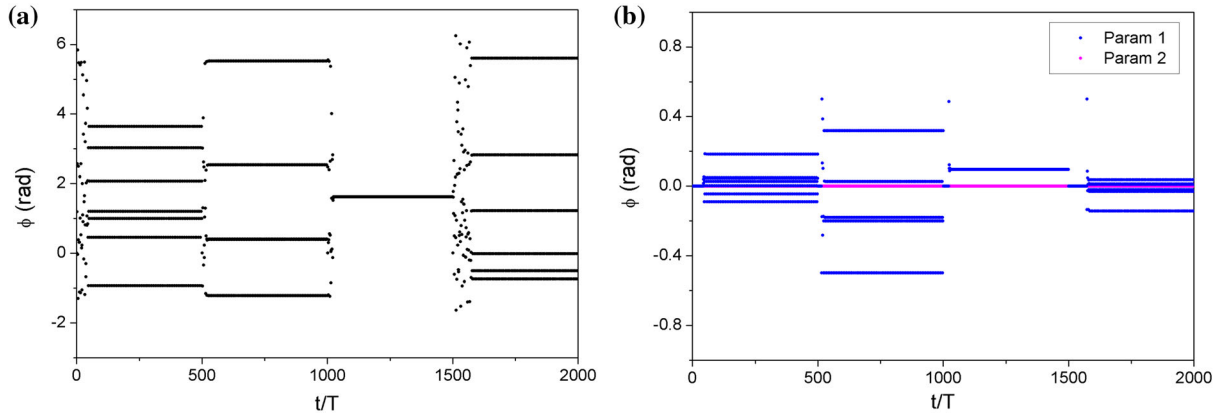

Fig. 6 System stabilization at S_1. **a** Position; **b** Control signal

with the determination of delay parameters: time delay, τ, and embedding dimension, D_e. The average mutual information method is an alternative to determine time delay [18] while the false nearest neighbors method is an option to estimate embedding dimension [30].

In terms of control purposes, it should be highlighted that the state space reconstruction by delay coordinates method causes the map F to be dependent on all control parameters perturbations performed in the time interval $t^n - \tau \leq t \leq t^{\,n}$ [15]. Thus, it is necessary to consider perturbations until δp^{n-r}, where r is the biggest value so that δp^{n-r} is inside the considered interval ($t^n - \tau \leq t \leq t^{\,n}$). Therefore, the use of states reconstructed by the method of delay coordinates implies that:

$$\xi^{n+1} = F(\xi^n, P^n, P^{n-1}, \ldots, P^{n-r}) \tag{13}$$

By considering the same steps previously employed, it is obtained:

$$\delta\xi^{n+1} = J^n \delta\xi^n + W_0^n \delta P^n + W_1^n \delta P^{n-1} + \cdots + W_r^n \delta P^{n-r} \tag{14}$$

where $J^n = D_{\xi^n} F(\xi_C^n, \delta P^n, \delta P^{n-1}, \ldots, \delta P^{n-r})$ and $w_i^n = D_{\delta p^{n-i}}(\xi_C^n, \delta P^n, \delta P^{n-1}, \ldots, \delta P^{n-r})$. By considering active and passive control parameters:

$$\delta\xi^{n+1} = J^n \delta\xi^n + W_{a0}^n \delta P_a^n + W_{p0}^n \delta P_p^n + W_{a1}^n \delta P_a^{n-1} + W_{p1}^n \delta P_p^{n-1} + \cdots + W_{ar}^n \delta P_a^{n-r} + W_{pr}^n \delta P_p^{n-r} \tag{15}$$

In order to obtain system stabilization, the same procedure presented at Sect. 2 must be considered and the vector $\delta\xi^{n+1}$ has to be aligned with the stable direction v_s^{n+1}.

3 Numerical simulations

As an application of the proposed chaos control procedure, a system with high instability characteristic is of concern. A nonlinear pendulum actuated by two different control parameters is considered as shown in Fig. 1. De Paula et al. [13] presented an experimental analysis of this pendulum, showing a mathematical model to describe the pendulum dynamical behavior. Basically, the pendulum consists of an aluminum disc with a lumped mass. An electric motor harmonically excites the pendulum via a string-spring device, which provides torsional stiffness to the system.

The mathematical model for the pendulum dynamics describes the time evolution of the angular position, ϕ, assuming that ϖ is the forcing frequency, I_D is the total inertia of rotating parts, k is the spring stiffness, ζ represents the viscous damping coefficient and μ the dry friction coefficient, m is the lumped mass, a defines the position of the guide of the string with respect to the motor, b is the length of the excitation arm of the motor, D is the diameter of the metallic disc and d is the diameter of the driving pulley. The equation of motion is given by [13]:

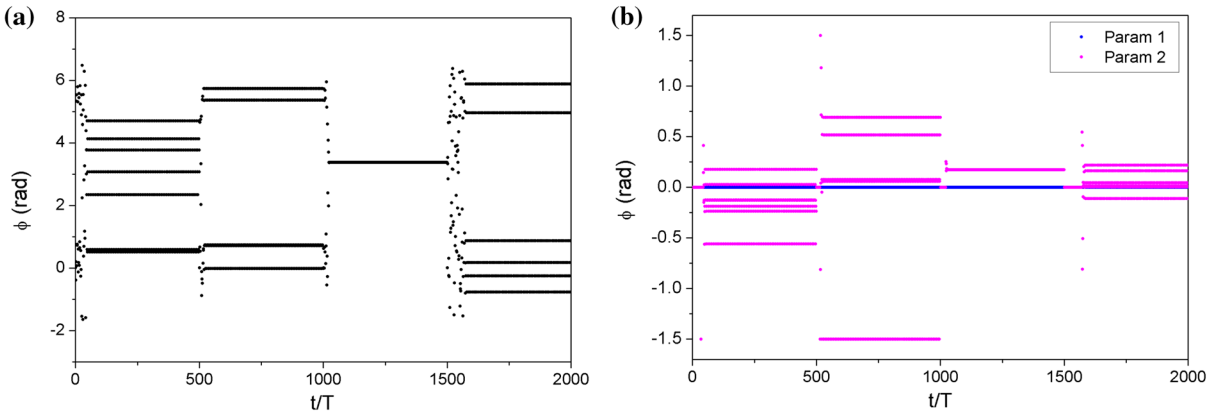

Fig. 7 System stabilization at S_2. **a** Position; **b** Control signal

$$\begin{Bmatrix} \dot{x}_1 \\ \dot{x}_2 \end{Bmatrix} = \begin{bmatrix} 0 & 1 \\ -\frac{kd^2}{2I_D} & -\frac{\zeta}{I_D} \end{bmatrix} \begin{Bmatrix} x_1 \\ x_2 \end{Bmatrix} + \left\{ 0 \frac{kd}{2I_D}(\Delta f(t) - \Delta l_1) - \frac{mgDsin(x_1)}{2I_D} - \frac{2\mu}{\pi I_D} atan(q x_2) \right\} \quad (16)$$

where

$$\Delta f(t) = \sqrt{a^2 + b^2 + \Delta l_2^2 - 2abcos(\varpi t) - 2b\Delta l_2 sin(\varpi t)} - (a - b)$$

and Δl_1 and Δl_2 correspond to actuations.

Numerical simulations of the pendulum dynamics are performed with the aid of the fourth-order Runge–Kutta method, being in close agreement with experimental data by assuming parameters used in [De Paula et al. [13]]: $a = 1.6 \times 10^{-1}$ m; $b = 6.0 \times 10^{-2}$ m; $d = 4.8 \times 10^{-2}$ m; $D = 9.5 \times 10^{-2}$ m; $m = 1.47 \times 10^{-2}$ kg; $I_D = 1.738 \times 10^{-4}$ kg m^2; $k = 2.47$ N/m; $\zeta = 2.386 \times 10^{-5}$ kg m^2 s^{-1}; $\mu = 1.272 \times 10^{-4}$ N m; $\varpi = 5.61$ rad/s.

Position and velocity time series are available from numerical integration of the mathematical model. By considering a situation where $\varpi = 5.61$ rad/s the system presents a chaotic behavior. Figure 2 presents phase space and Poincaré section showing the chaotic behavior of the pendulum.

A scalar time series of angular position is assumed as representative of system dynamics, being acquired with sampling time $2\pi/(120\varpi)$, where ϖ is the forcing frequency. For $\varpi = 5.61$ rad/s, the sampling time is $\tau_S \approx 9.3 \times 10^{-3}$ s. In order to reconstruct the system dynamics from time series, the method of delay coordinates is employed. The average mutual information method is employed to determine time delay while the false nearest neighbors method is used to estimate embedding dimension. Thus, κ is determined by analyzing the information curve, being defined by the minimum value of $I(\kappa)$ curve, shown in Fig. 3a. Embedding dimension, D_e, is determined by choosing a situation where the false nearest neighbors percentage is approximately zero (Fig. 3b). Therefore, Fig. 3 indicates that $\kappa \approx 32$ (meaning that time delay is and $D_e = 3$). Figure 4 shows the reconstructed state space and Poincaré section related to chaotic behavior, employing these delay parameters. A comparison between reconstructed state space (Fig. 4) with the real state space (Fig. 2) shows that both responses have the same characteristics, preserving the dynamics aspects.

At this point, the capability of the uncoupled approach of the SC-MP to stabilize UPOs using delay coordinates reconstruction is of concern. The first step is the identification of UPOs embedded in chaotic attractor, which is done by using the close return method [3]. Four control sections (S_1, S_2, S_3 and S_4), uniformly distributed in one forcing period, are considered. Moreover, once the signal is sampled 120 times per forcing cycle, the time interval between two consecutive control sections, τ_Σ, correspond to 30 samples, $\tau_\Sigma = 30\tau_s$. On the other hand, the time delay

is $\tau = 32\tau_s$. Thus, to include all control parameters influence in the interval $t^n - 32\tau_s \leq t \leq t^n$ it is necessary to consider the perturbations δP^n, δP^{n-1} and δP^{n-2}. This implies that only sensitivity matrixes W_0^n, W_1^n and W_2^n should be determined during the learning stage. If τ is smaller than τ_Σ, only the influence of δP^n and δP^{n-1} is enough.

A control rule is defined for the stabilization of four different identified UPOs, in the following sequence: a period-7 orbit during the first 500 periods, a period-5 from period 500 to 1,000, a period-1 from 1,000 to 1,500 and, finally a period-6, from period 1,500 to 2,000. Maximum perturbation of $|\Delta l_{1\max}| = 5$ mm and $|\Delta l_{2\max}| = 15$ mm are assumed with reference position being $\Delta l_{10} = \Delta l_{20} = 0$ mm. Figure 5 presents the UPOs of the control rule at the considered control sections S_1, S_2, S_3 and S_4.

After determining the fixed points of the UPOs at control sections, the local dynamics expressed by the Jacobian matrix and the sensitivity matrix of each fixed points at each control station are determined using the least-square fit method [3, 24].

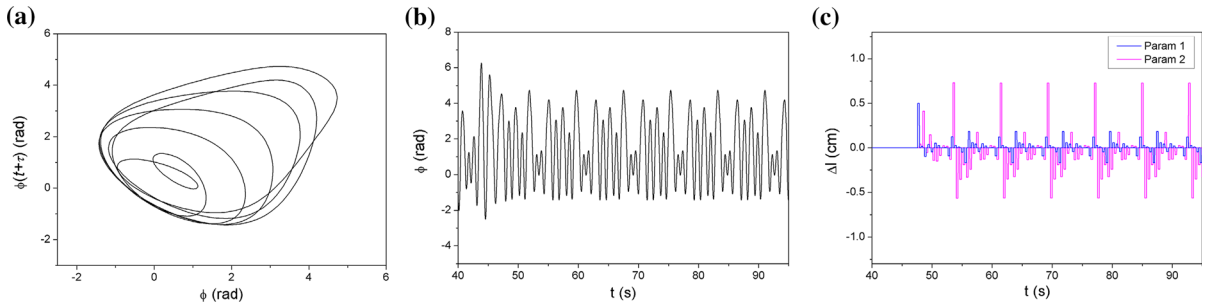

Fig. 8 Period-7 UPO stabilization details: **a** Phase space; **b** Position; **c** Perturbations

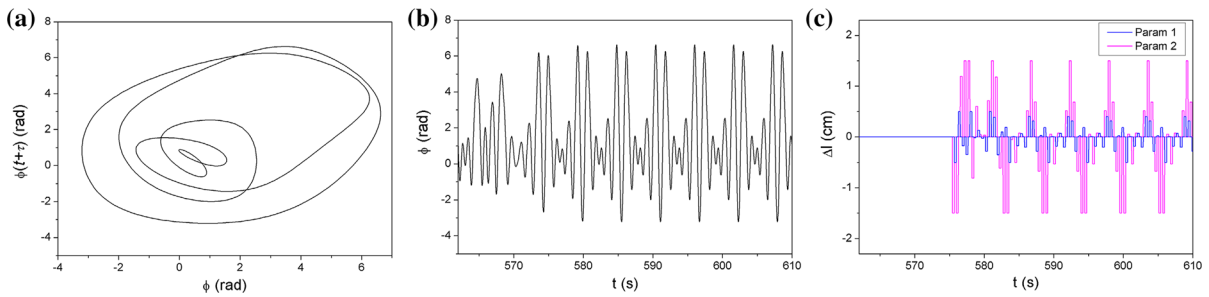

Fig. 9 Period-5 UPO stabilization details: **a** Phase space; **b** Position; **c** Perturbations

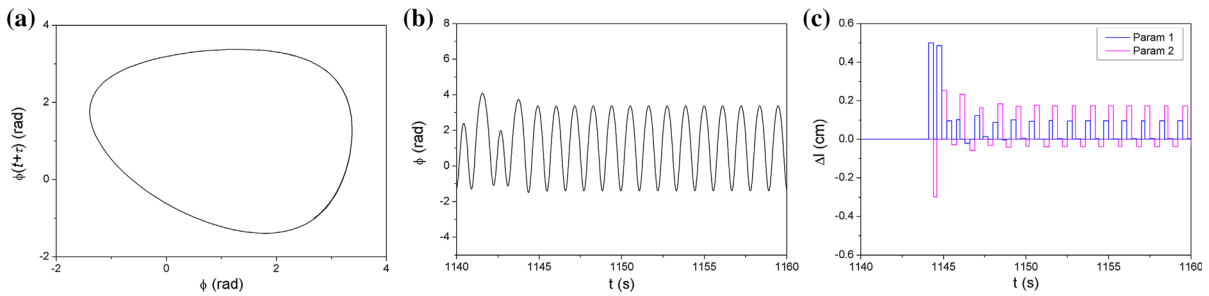

Fig. 10 Period-1 UPO stabilization details: **a** Phase space; **b** Position; **c** Perturbations

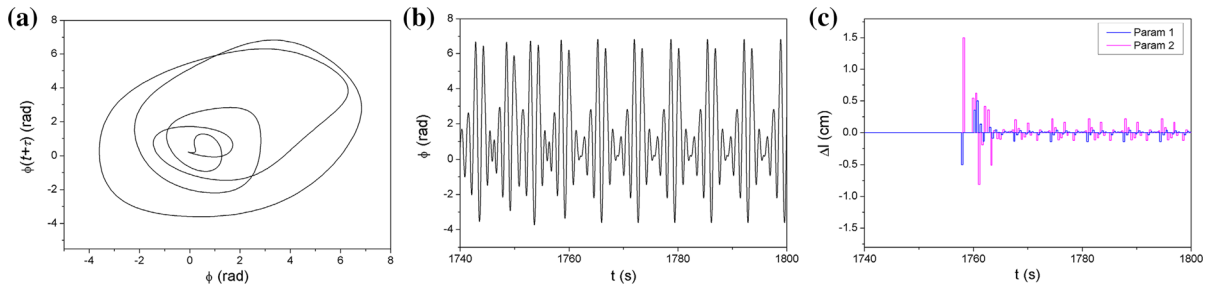

Fig. 11 Period-6 UPO stabilization details: **a** Phase space; **b** Position; **c** Perturbations

Sensitivity matrixes W_0^n, W_1^n and W_2^n are estimated by the procedure described in Dressler and Nitsche [15]. After that, the SVD technique is employed for determining the stable and unstable directions near the next fixed point. After the learning stage, the control stage starts.

Figures 6 and 7 present the controller performance related to the established control rule for two different control stations, S_1 and S_2, respectively. Each of these Figures presents system time evolution and the actuators behavior. Results show that this control approach is effective to stabilize all orbits of the control rule.

Details of the stabilized UPOs of the control rule, periodicity 7, 5, 1 and 6, are presented in Figs. 8, 9, 10, 11, respectively, showing the phase space, temporal evolution of pendulum position and control perturbations. It can be observed that the controller is able to stabilize all UPOs of the control rule. Moreover, after a transient time the perturbation values become periodic. It is also noticeable that both control parameters are employed during actuation process.

The obtained results show that it is possible to achieve the stabilization of UPOs from scalar time series by employing the uncoupled approach of the MP-SC using delay coordinates to reconstruct system dynamics.

4 Conclusions

This contribution discusses the application of the state space reconstruction on the uncoupled approach of the semi-continuous multiparameter method for chaos control. The method of delay coordinates is employed to reconstruct system dynamics. Therefore, it is necessary to consider the effect of all control parameters perturbations performed in delayed states. The formulation of the actuation process for these conditions is presented. As an application of the general formulation, a two-parameter control of a nonlinear pendulum is treated. The stabilization of some identified UPOs is successfully achieved showing the possibility of using such approach to control chaotic behavior of mechanical systems. The use of delay coordinates for state space reconstruction allows the application of chaos control from time series analysis.

Acknowledgments The authors would like to acknowledge the support of the Brazilian Research Agencies CNPq, CAPES and FAPERJ and through the INCT-EIE (National Institute of Science and Technology—Smart Structures in Engineering) the CNPq and FAPEMIG. The Air Force Office of Scientific Research (AFOSR) is also acknowledged.

References

1. Andrievskii BR, Fradkov AL (2004) Control of chaos: methods and applications. II. Applications. Autom Remote Control 65(4):505–533
2. Arecchi FT, Boccaletti S, Ciofini M, Meucci R (1998) The control of chaos: theoretical schemes and experimental realizations. Int J Bifurc Chaos 8(8):1643–1655
3. Auerbach D, Cvitanovic P, Eckmann J-P, Gunaratne G, Procaccia I (1987) Exploring chaotic motion through periodic orbits. Phys Rev Lett 58(23):2387–2389
4. Barreto E, Grebogi C (1995) Multiparameter control of chaos. Phys Rev E 54(4):3553–3557
5. Bessa WM, de Paula AS, Savi MA (2009) Chaos control using an adaptive fuzzy sliding mode controller with application to a nonlinear pendulum. Chaos Solitons Fractals 42(2):784–791
6. Bessa WM, de Paula AS, Savi MA (2012) Sliding mode control with adaptive fuzzy dead-zone compensation for uncertain chaotic systems. Nonlinear Dyn 70(3):1989–2001
7. Bessa WM, de Paula AS, Savi MA (2013) Adaptive fuzzy sliding mode control of a chaotic pendulum with noisy signals. ZAMM J Appl Math Mech. doi:10.1002/zamm.201200214

8. de Korte RJ, Schouten JC, van den Bleek CMV (1995) Experimental control of a chaotic pendulum with unknown dynamics using delay coordinates. Phys Rev E 52(4):3358–3365
9. De Paula AS, Savi MA (2008) A multiparameter chaos control method applied to maps. Braz J Phys 38(4):537–543
10. De Paula AS, Savi MA (2009) A multiparameter chaos control method based on OGY approach. Chaos Solitons Fractals 40(3):1376–1390
11. De Paula AS, Savi MA (2009) Controlling chaos in a nonlinear pendulum using an extended time-delayed feedback control method. Chaos Solitons Fractals 42(5):2981–2988
12. De Paula AS, Savi MA (2011) Comparative analysis of chaos control methods: a mechanical system case study. Int J Non-Linear Mech 46(8):1076–1089
13. De Paula AS, Savi MA, Pereira-Pinto FHI (2006) Chaos and transient chaos in an experimental nonlinear pendulum. J Sound Vib 294(3):585–595
14. De Paula AS, Savi MA, Wiercigroch M, Pavlovskaia E (2012) Bifurcation control of a parametric pendulum. Int J Bifurc Chaos 22(5):1–14, Article 1250111
15. Dressler U, Nitsche G (1992) Controlling chaos using time delay coordinates. Phys Rev Lett 68(1):1–4
16. Ferreira BB, de Paula AS, Savi MA (2011) Chaos control applied to heart rhythm dynamics. Chaos Solitons Fractals 44(8):587–599
17. Fradkov AL, Evans RJ, Andrievsky BR (2006) Control of chaos: methods and applications in mechanics. Phylos Trans R Soc 364:2279–2307
18. Fraser AM, Swinney HL (1986) Independent coordinates for strange attractors from mutual information. Phys Rev A 33:1134–1140
19. Grebogi C, Lai Y-C (1997) Controlling chaotic dynamical systems. Syst Control Lett 31:307–312
20. Hübinger B, Doerner R, Martienssen W, Herdering M, Pitka R, Dressler U (1994) Controlling chaos experimentally in systems exhibiting large effective Lyapunov exponents. Phys Rev E 50(2):932–948
21. Kapitaniak T (1992) Controlling chaotic oscillators without feedback. Chaos Solitons Fractals 2(5):512–530
22. Kapitaniak T (2005) Controlling chaos: theoretical and practical methods in non-linear dynamics. Academic Press Inc, San Diego
23. Ogorzalek M (1994) Chaos control: how to avoid chaos or take advantage of it. J Franklin Inst 331B(6):681–704
24. Otani M, Jones AJ (1997) Guiding chaotic orbits Research Report—Imperial College of Science Technology and Medicine, London
25. Ott E, Grebogi C, Yorke JA (1990) Controlling chaos. Phys Rev Lett 64(11):1196–1199
26. Pereira-Pinto FHI, Ferreira AM, Savi MA (2004) Chaos control in a nonlinear pendulum using a semi-continuous method. Chaos Solitons Fractals 22(3):653–668
27. Pereira-Pinto FHI, Ferreira AM, Savi MA (2005) State space reconstruction using extended state observers to control chaos in a nonlinear pendulum. Int J Bifurc Chaos 15(12):4051–4063
28. Pyragas K (1992) Continuous control of chaos by self-controlling feedback. Phys Lett A 170:421–428
29. Pyragas K (2006) Delayed feedback control of chaos. Phylos Trans R Soc 364:2309–2334
30. Rhodes C, Morari M (1997) False-nearest-neighbors algorithm and noise-corrupted time series. Phys Rev E 55(5):6162–6170
31. Ritz T, Schweinsberg ASZ, Dressler U, Doerner R, Hübinger B, Martienssen W (1997) Chaos control with adjustable control times. Chaos Solitons Fractals 8(9):1559–1576
32. Savi MA (2006) Nonlinear dynamics and chaos, Editora E-papers (in portuguese)
33. Shinbrot T, Grebogi C, Ott E, Yorke JA (1993) Using small perturbations to control chaos. Nature 363:411–417
34. So P, Ott E (1995) Controlling chaos using time delay coordinates via stabilization of periodic orbits. Phys Rev E 51(4):2955–2962
35. Socolar JES, Sukow DW, Gauthier DJ (1994) Stabilizing unstable periodic orbits in fast dynamical systems. Phys Rev E 50(4):3245–3248
36. Yanchuk S, Kapitaniak T (2001) Symmetry-increasing bifurctaion as a predictor of a chaos-hyperchaos transition in coupled systems. Phys Rev E 64(056235):1–5
37. Yanchuk S, Kapitaniak T (2001) Chaos-hyperchaos transition in coupled Rossler systems. Phys Lett A 290:139–144